

# Ultra-thin SiO<sub>2</sub> on Si VIII. Accuracy of method, linearity and attenuation lengths for XPS

Kyung Joong Kim<sup>1</sup> and M. P. Seah<sup>2\*</sup>

<sup>1</sup> Division of Advanced Technology, Korea Research Institute of Standards and Science (KRISS), Yusong, Taejeon 305-600, Korea

<sup>2</sup> Quality of Life Division, National Physical Laboratory, Teddington, Middlesex TW11 0LW, UK

Received 7 September 2006; Accepted 30 November 2006

In the study of ultra-thin films (<10-nm thick), there is a range of methods that can provide accurate measurements of differences in thickness. However, in a pilot study under the auspices of the Consultative Committee for Amount of Substance (CCQM), results for the archetypal system of SiO<sub>2</sub> on Si show that the methods have different offsets such that, at all thicknesses, positive or negative amounts in the range up to 1 nm may be observed between methods. All the methods studied give thicknesses that are greater than those measured by X-ray photoelectron spectroscopy (XPS) by amounts between 0.2 nm and approximately 1 nm. Significant parts of these offsets, of other methods with respect to XPS, may be attributed to contaminations which increase the apparent thickness but that do not affect XPS. However, not all of these offsets can yet be explained at the 0.2 nm level. The remaining part of the offsets could be thought to have arisen either from the XPS or from the other methods. In this study, by measuring SiO<sub>2</sub> deposited *in situ* on amorphous Si by XPS it is shown that the XPS linearity is consistent with the previous estimate of  $\pm 0.025$  nm, down to fractions of a monolayer, with no significant offset and that, therefore, it is the offsets seen using other methods that need further study. Recent calculations of the film thickness dependence of the attenuation lengths (ALs) for this system, using NIST SESSA software, are not consistent with these data although earlier calculations are. This work shows that XPS, with the AL calibrated by one or more other methods that are valid for differences in thickness, can provide a traceable measurement of thickness in all laboratories. © Crown Copyright 2007. Reproduced with the permission of Her Majesty's Stationery Office. Published by John Wiley & Sons, Ltd.

**KEYWORDS:** attenuation lengths; calibration; linearity; silicon oxide; XPS

## INTRODUCTION

The measurement of the thicknesses of films in the range up to 10 nm has been made using X-ray photoelectron spectroscopy (XPS) since the late 1960s. Many other measurement methods are sensitive to ultra-thin films. These can accurately measure the differences in thickness between samples in sets of such films but most of these methods either determine the total thickness including any contaminations or determine the thickness for a particular element rather than for that element in a given chemical state.

The true, length-determining methods are usually traceable to the metre by simple and clear measurement chains. If these need to be converted to amount of substance in mass per unit area, which may be more meaningful at thicknesses below 1 nm, an estimate of the density is required. For some analytical methods, where the signal is related to the number of atoms of a given element, a direct result can be in atoms or mass per unit area and can be converted to thickness, in metres, if an estimate of the density is available.

The problem for many methods is that the samples to be characterised may have adventitious contamination that covers the layer to be measured. This adventitious contamination will usually include hydrocarbons and water for samples that are otherwise relatively inert in the ambient environment. These contaminations may be in excess of 0.2 and 0.3 nm, respectively,<sup>1</sup> for relatively clean samples analysed in vacuum. The contaminations may grow or change in composition during analysis with the various methods. These contamination levels are very small but are significant in the present set of studies where layers of SiO<sub>2</sub> on Si in the range of up to 8 nm are measured. The contaminations may add physically to the apparent thickness or, if the oxygen amount is analysed, oxygen atoms in the water and/or in the carbonaceous contamination, will be included.

The above effects were shown in a recent pilot study under the auspices of the Consultative Committee for Amount of Substance (CCQM).<sup>1</sup> In that work, by plotting the thicknesses of SiO<sub>2</sub> measured by each method *versus* that determined by XPS, excellent correlations were obtained but with many of the methods giving a small, constant excess or offset with respect to the XPS. The different methods had different offsets in the range from 0.2 nm to approximately

\*Correspondence to: M. P. Seah, Quality of Life Division, National Physical Laboratory, Teddington, Middlesex TW11 0LW, UK.  
E-mail: Martin.Seah@npl.co.uk

1 nm. Significant parts of these offsets may be attributed to contamination layers but not all offsets could be explained at the 0.2 nm level. The remaining part of the offsets could be thought to have arisen either from the XPS or the other methods. It is this linearity and concern for any offset in XPS measurements for the thicknesses of SiO<sub>2</sub> on Si that is the focus of the present study.

XPS measurements of thickness are insensitive to the layers of contamination for analysis of oxide layers on substrates when measuring, as in the SiO<sub>2</sub> on Si case considered here, the substrate element in the elemental and oxide states. Thus, this approach is particularly good for gate oxides and extensive tests have been made for SiO<sub>2</sub> on Si in the range of 1.5–8 nm.<sup>1</sup> In this mode, the thickness  $d$  is given by the simple equation:

$$d = L \cos \theta \ln(1 + R/R_0) \quad (1)$$

where  $L$  is the attenuation length (AL) for the analysed electrons in the overlayer (here, for Si 2p electrons in the SiO<sub>2</sub>),  $\theta$  is the angle of emission of the detected electrons from the surface normal (analysers should accept  $\pm 6^\circ$  or lower cone semi-angle of electrons<sup>2</sup>),  $R$  is the ratio of the intensities,  $I_{\text{SiO}_2}$  and  $I_{\text{Si}}$ , for the element in the oxide and elemental states respectively, and  $R_0$  is the equivalent ratio of intensities,  $I_{\text{SiO}_2}^\infty$  and  $I_{\text{Si}}^\infty$ , from bulk oxide and substrate, respectively.<sup>3</sup> In practice, for SiO<sub>2</sub> on Si, we use four equations like Eqn (1), but one is sufficient for the present discussion. If  $L$  can be calibrated, as it was in the pilot study,<sup>1,3</sup> these equations are accurately quantitative for the measurement of thickness. If the film is not of a compound of a pure element that forms the substrate, the equations become more complex and have greater uncertainties<sup>4</sup> some of which then need to include effects for contamination. Measurements for SiO<sub>2</sub> on Si using the Si 2p electron intensities for the oxide and elemental substrate confirm, however, that Eqn (1) is insensitive to contamination for levels far in excess of the levels to be considered here.<sup>5</sup>

In general, Eqn (1) may be used with  $L$  calculated from the inelastic mean free path<sup>6</sup> reduced to allow for elastic scattering.<sup>6,7</sup> For most practical measurement conditions, the reduction factor is around 0.9 but may be calculated reasonably accurately. The calculated inelastic mean free path, however, is estimated to be accurate to only 20%.<sup>8</sup> Furthermore, both the calculated adjustment for elastic scattering<sup>9</sup> and the inelastic mean free path<sup>10–13</sup> may be dependent on the film thickness  $d$  so that, to some extent, Eqn (1) becomes non-linear. If this is significant, the non-linearity in Eqn (1) may need to be calibrated for each material system and geometry or be included in the uncertainty attributed to the analysis. It is this non-linearity that we shall evaluate in the current study, extending the previous work<sup>1–3,5</sup> for SiO<sub>2</sub> on Si. It may well be that, even if this material system is linear, significant non-linearity may occur with other systems such as those involving metallic or high atomic number overlayers.

The measurement of SiO<sub>2</sub> on Si by XPS has been covered in some detail in earlier publications.<sup>1–3,5,7,14</sup> In those studies, thermal oxides were grown in equipment designed for pilot scale gate oxide preparation using oxygen at elevated

temperatures.<sup>1</sup> The wafers with the oxide were then cleaved to suitable sizes for analysis by XPS and other methods. This procedure, conducted in air, leaves all samples with some contamination but, if the samples are stored carefully in appropriate containers, levels may be maintained at around 0.2–0.3 nm for the carbonaceous contamination,<sup>14</sup> and about one monolayer for the water. Furthermore, oxide thicknesses below 1 nm were thought to be unstable in air and so 1.5 nm was used as a lower limit. In practice, it was later found that oxide films as thin as 0.8 nm could be stable in air for >2 years.

In recent work, one of us has demonstrated an alternative production route for SiO<sub>2</sub> on Si that allows a closer study of the linearity of Eqn (1). This involves films deposited *in situ* and analysed by XPS,<sup>15</sup> as discussed below. By depositing the films on amorphous Si substrates, the forward focusing issues are removed so that any azimuth and reasonable emission angle,  $\theta$ , may be used. By using ultra-high vacuum ion beam sputter deposition<sup>16</sup> and *in situ* XPS, the effects of the contaminants are eliminated but, more critically, films significantly below 1 nm that are unstable in air, may be studied in order to evaluate the linearity down to fractional monolayers.

## EXPERIMENTAL

SiO<sub>2</sub> films were grown by reactive ion beam sputter deposition using a Kaufman type direct current (DC) ion gun in the ion beam-assisted sputter deposition system described by Kim and Moon<sup>17</sup> and shown in Fig. 1. First, the Si target was sputtered with 750 eV Ar ions in UHV to cover an n-type Si (100) wafer with a thick layer of amorphous Si at room temperature. This sample was then transported in UHV for XPS analysis. The XPS system uses a VSW HAC 5000 XPS spectrometer with Mg K $\alpha$  X-rays at 1254 eV photon energy. The spectrometer had a nominal resolution of 1 eV at 10 eV pass energy. No argon contamination was visible in the XPS data for this deposit. The sample was then returned to the deposition chamber and a fresh layer of Si was deposited, followed directly by argon sputtering the Si target for a fixed time,  $t$ , in an oxygen environment at  $2.7 \times 10^{-4}$  mbar. These conditions deposit a very thin layer of stoichiometric SiO<sub>2</sub> on top of the amorphous Si layer. The deposition time was accurately defined by switching on the ion beam with a voltage rather than switching on the whole ion gun. This time was estimated to have an uncertainty of 0.1 s. The surface was then analysed again by XPS.

Measurements were made after 10 depositions of the amorphous Si substrate layer, each followed by successively longer choices of the time  $t$  of depositions of SiO<sub>2</sub> up to a maximum of 50 s. The first value of  $t$  is zero but the cycle of operations is the same as that for a non-zero time in order to measure the oxide arising from the background oxygen pressure and the gas admission before the start of the sputter deposition of the SiO<sub>2</sub>. Two sets of data were recorded in this way and one further set with only seven cycles of measurement. The first set comprised a series of XPS measurements at an emission angle of  $10^\circ$ , to be consistent with earlier work using this equipment.<sup>15</sup> The

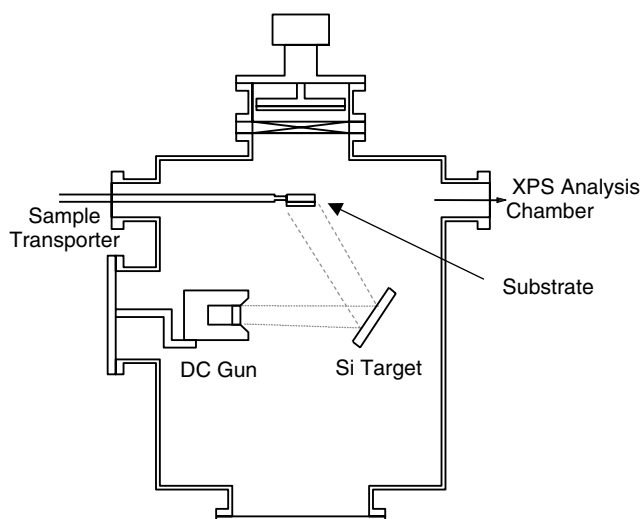


**Figure 1.** Schematic of the ion beam deposition system used for Si and SiO<sub>2</sub>, attached to the XPS analysis system, after Kim and Moon.<sup>17</sup>

second involved a series of measurements at 10°, 25.5° and 34° emission angles, in that sequence, for each deposited film thickness. The 25.5° and 34° emission angles are the reference geometry for the studies in Refs 1–3, 5. Finally, the conditions of the first set were repeated but for deposition times from 0 to 6 s with the increments reduced to 1 s. The emission angles were all set to within 0.5°.

Figure 2 shows the first set of spectra recorded for an emission angle of 10°. As previously, these spectra then have the X-ray satellites removed together with the 2p<sub>3/2,1/2</sub> spin-orbit splitting determined as 50% of the intensity at 0.60 eV higher binding energy (BE).<sup>18</sup> The remaining structure was evaluated as 5 peak intensities,  $I_{Si}$ ,  $I_{Si_2O}$  at 0.95 eV higher BE,  $I_{SiO}$  at 1.75 eV higher BE,  $I_{Si_2O_3}$  at 2.48 eV higher BE and  $I_{SiO_2}$  at 3.90 to 4.50 eV higher BE, approximately, as defined by Hollinger and Himpfel<sup>18</sup> and by Keister *et al.*<sup>19</sup> These peaks were fitted with the peak positions fixed in relation to the Si peak, as indicated, except for the SiO<sub>2</sub> peak which was allowed to move to higher BEs as the film thickness increased. The peak fitting was simultaneous with the removal of a Shirley background<sup>20</sup> using a 21-point smooth, inwards from the end points at 8.9 eV higher and 3.6 eV lower BE than the Si 2p peak. This smooth defines the background more precisely.<sup>2</sup> All peak FWHMs were constrained to be in the range of 0.7–1.5 eV with the latter extended, for SiO<sub>2</sub>, to 1.7 eV.

To determine the total film thickness, as noted earlier, Eqn (1) is replaced by four equations<sup>1,21</sup> to include, specifically, the interfacial oxides, Si<sub>2</sub>O<sub>x</sub>. These equations are:

$$d_{SiO_2} = L_{SiO_2} \cos \theta \ln \left[ 1 + \frac{\left( \frac{I_{SiO_2}}{R_{SiO_2}} \right)}{\left( \frac{I_{Si_2O_3}}{R_{Si_2O_3}} + \frac{I_{SiO}}{R_{SiO}} + \frac{I_{Si_2O}}{R_{Si_2O}} + I_{Si} \right)} \right] \quad (2)$$

$$d_{Si_2O_3} = L_{Si_2O_3} \cos \theta \ln \left[ 1 + \left( \frac{I_{Si_2O_3}}{R_{Si_2O_3} I_{Si}} \right) \right] \quad (3)$$

$$d_{SiO} = L_{SiO} \cos \theta \ln \left[ 1 + \left( \frac{I_{SiO}}{R_{SiO} I_{Si}} \right) \right] \quad (4)$$

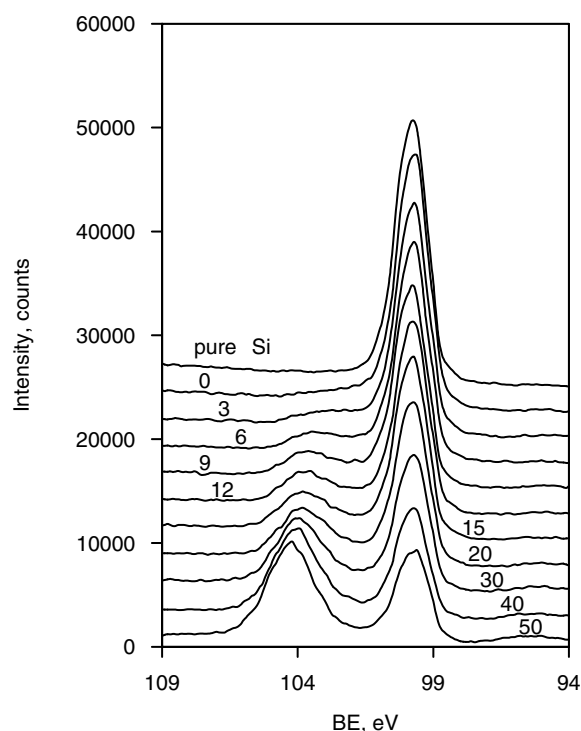


**Figure 2.** Si 2p XPS spectra using Mg K $\alpha$  X-rays, at 10° emission angle, for ion beam deposited SiO<sub>2</sub> films. The different spectra are for different nominal thicknesses derived from the deposition times given above each curve in seconds (50 s ~ 3 nm).

and

$$d_{Si_2O} = L_{Si_2O} \cos \theta \ln \left[ 1 + \left( \frac{I_{Si_2O}}{R_{Si_2O} I_{Si}} \right) \right] \quad (5)$$

These thicknesses are then summed to give the effective oxide thickness using the equation

$$d_{oxide} = d_{SiO_2} + 0.75 d_{Si_2O_3} + 0.5 d_{SiO} + 0.25 d_{Si_2O} \quad (6)$$

which apportions the thickness according to the oxygen content.

The values of  $L_{Si_2O_x}$  and  $R_{Si_2O_x}$  are determined by linear interpolation between the values for SiO<sub>2</sub> and Si depending on the value of  $x$ .<sup>21</sup>

## RESULTS AND DISCUSSION

Figure 3 shows a plot of the thicknesses determined by XPS for the first 10° emission data-set, using Eqns (2)–(6), as a function of the deposition time. From the earlier study,<sup>15</sup> 50 s of deposition gave around 3 nm of oxide. In work on thermal oxides, the value of  $R_o$  of 0.9329 is used.<sup>1,21</sup> We have checked the effect of varying  $R_o$  in the range of 0.88–0.933 and found that this alters  $d$  by  $\pm 1.8\%$  about the average but that the accuracy of the nominal thickness conversion is insufficient to test which absolute values are correct for this material. For the present purposes of evaluating the linearity, this choice is unimportant and so we use 0.9329. Here, we have used  $L_{SiO_2} = 2.996$  nm for Mg X-rays, as determined from the

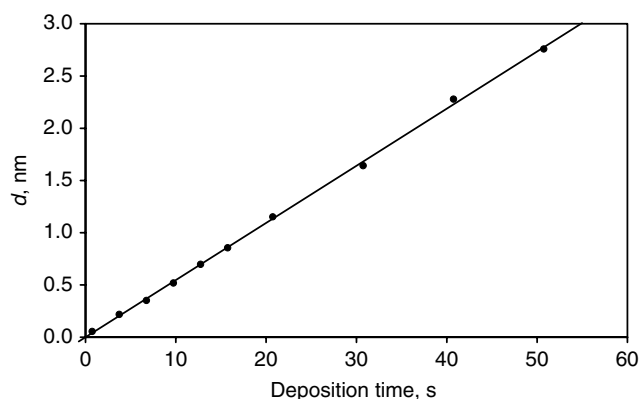


**Figure 3.** Thickness measured by XPS for an emission angle of 10° as a function of the time of deposition of the SiO<sub>2</sub> layer (the first set of data).

detailed pilot study for thermal oxides.<sup>3</sup> Again, the choice is unimportant here but this value is used for consistency.

What is important is the linearity of the plot in Fig. 3. The XPS analysis at  $t = 0$  shows, before deposition from the sputter source, a very small amount of oxidation caused by the oxygen present between depositing the Si substrate and turning on the sputtering beam to deposit the SiO<sub>2</sub> layers. As can be seen in Fig. 2, this is mostly Si<sub>2</sub>O and amounts to a layer equivalent to 0.041 nm of SiO<sub>2</sub> from the above equations. This is not the result of poor fitting to a tail to the Si peak since the first analysis, shown in Fig. 2, is for the pure Si substrate which exhibits an oxide signal equivalent to <0.001 nm of SiO<sub>2</sub>. It will be remembered that the total equivalent thickness of the intermediate oxides in SiO<sub>2</sub> was  $0.128 \pm 0.008$  nm for the thermal oxides.<sup>1</sup> This interfacial oxide thickness is equivalent to the thickness that would result from a flat slab of SiO<sub>2</sub> in intimate contact with a flat slab of Si. Thus, any layer of <0.128 nm thickness will be expected to be for the intermediate oxide states, as seen here. The starting level of oxide is approximately equivalent to 15% of a monolayer of chemisorbed oxygen and shows exceptionally good control of the environment in these difficult experiments.

Of course, XPS has been used for about 30 years in the study of the initial stages of oxidation without anomalous results being found. Partial monolayers are analysed by XPS without any significant incubation quantity or offset. Thus, using Eqns (2)–(6), the initial value of 0.041 nm will be valid and, even if the dependence of the AL on film thickness is as high as 10%, the absolute uncertainty on such a small thickness will be only 0.004 nm. This is significantly less than the measurement uncertainty generally arising from the repeatability contribution for the remaining data and so is considered to be negligible here. Thus, Fig. 3 shows the thickness determined by XPS using a constant AL *versus* the deposition time. To allow for the first deposit of 0.041 nm discussed above, a fixed time of 0.7 s has been added as a prior exposure time to all of the deposition times used. Figure 3 allows us to investigate the departure from linearity. This departure is shown in Fig. 4. This result is extremely insensitive to the values of  $R_0$  and  $L$  used. For values of  $R_0$  in the range of 0.88–0.9329, the average

standard deviation of the points for each film thickness in Fig. 4 is 0.001 nm. The choice of  $L$  does not affect the linearity of the data in Fig. 3. The data in Figs 3 and 4 show no significant variations from a linear result within the experimental scatter. The experimental scatter here has contributions from the analytical counting statistics<sup>2</sup> (e.g. 0.01 nm at 3 nm), the ion gun beam stability (1% standard deviation), the exposure time for deposition and the resetting of the angle of emission for each measurement. In the exposure time, there is a 0.1 s standard uncertainty in each of the exposures and, in resetting the angle of emission, there is a 0.5° angular uncertainty for each measurement. These uncertainties generate the 95% uncertainty error bars shown in Fig. 4.

In the second run, using the three different emission angles, the results shown in Fig. 5 were obtained using  $L = 2.996$  nm. Here, the abscissa has been converted to thickness using a proportionality constant chosen to set the gradient of the linear regression line to unity. The value of this constant is unimportant. It does not affect the expression of the linearity or any offset, which are given in units of the ordinate. For clarity, only the average XPS thicknesses are plotted on the ordinate. The data points for the three angles are very consistent and exhibit an average scatter standard deviation of 0.023 nm from the averages shown. The standard deviation for each thickness is indicated by an error bar. The initial value in this set was 0.058 nm, slightly higher than before but, even if the AL varies by 10% for different thicknesses of film, the error here will only be 0.006 nm. The 0.058 nm has been included in the abscissa values.

In the third run, the region around the origin in Fig. 3 was studied more carefully. The method used, of redepositing the Si substrate each time, stops the uncertainty in the total deposition time from increasing with thickness. The use of an emission angle of 10° reduces the impact of the 0.5° angular uncertainty. This set of data was recorded with great care and led to a plot like Fig. 3 but with the offset at  $t = 0$  reduced to 0.022 nm, equivalent to only 8% of a monolayer

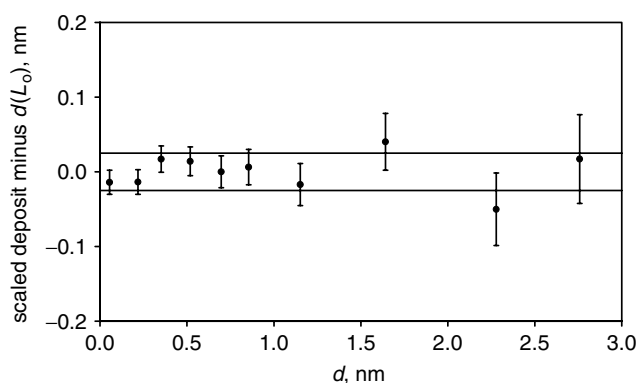


**Figure 4.** Departure from linearity, as measured by the thickness from the scaled deposition time minus the thickness for the XPS data with a constant AL at an emission angle of 10°, together with error bars showing the uncertainties involving both the deposition exposures and the uncertainties of the XPS measurement. The horizontal lines show the previously estimated<sup>21</sup> uncertainty limits of  $\pm 0.025$  nm.

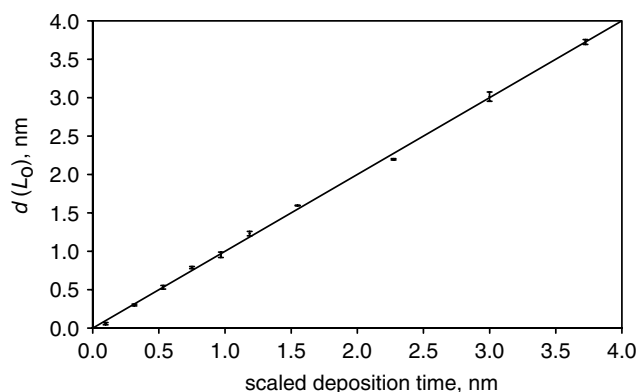


**Figure 5.** Average thickness increase,  $d(L_o)$ , measured by XPS for  $10^\circ$ ,  $25^\circ$  and  $34^\circ$  emission angles as a function of the thickness calculated by scaling the deposition time for the  $\text{SiO}_2$  layer (the second set of data). The error bars show the standard deviations of the three sets of XPS measurements.

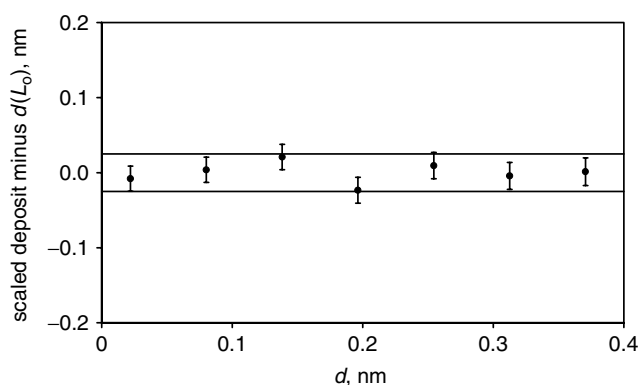


**Figure 6.** Departure from linearity, as plotted in Fig. 4 for an emission angle of  $10^\circ$ , together with error bars and uncertainty limits of  $\pm 0.025$  nm as in Fig. 4 (the third set of data).

of oxygen arising from exposures other than those during the timed deposition. The departure from linearity, in the form of Fig. 4 with the same error contributions, is shown in Fig. 6. The linearity appears to be upheld within the original estimate of  $\pm 0.025$  nm. The standard deviation of the points about zero is a remarkable 0.014 nm.

These data show that XPS is linear for the system of  $\text{SiO}_2$  on Si as presented and used here. The use of a constant value of the AL,  $L_o$ , independent of film thickness, is upheld within the measurement uncertainty. This is an important point to establish since there is no reason for the AL to be exactly constant. The offsets seen in the other methods of measurement used in the CCQM pilot study<sup>1</sup> cannot arise from a non-linearity of the XPS, and hence, other sources for the offsets need to be found. These offsets were largely explained in Ref. 1 as resulting from contaminant layers that add to the thicknesses measured in many of the other methods, but some offsets up to 0.2 nm remained unexplained and, without the present data, it could be argued that the XPS measurements, used with a fixed AL, generate thicknesses that are progressively too low for the thinner samples by this amount. What are the effects of a film-thickness-dependent AL? Over recent years, Powell and co-workers have made a number of

predictions concerning the film-thickness-dependence of the AL that will be briefly reviewed here.

The first calculations for the variation of the AL,  $L(d)$ , with film thickness by Powell and Jablonski in 2001<sup>22</sup> show consistency with the present results within the experimental scatter. Note that the AL here is the same as the effective attenuation length (EAL) term used by Powell and Jablonski except that the present AL is defined from Eqn (1), whereas that of Powell and co-workers is from

$$d(L) = L \cos \theta \ln(I_{\text{Si}}^\infty / I_{\text{Si}}) \quad (7)$$

We will retain this distinction by retaining Powell's term of EAL for this approach that only uses the substrate signal. In practice, of course, experimentalists generally do not know  $I_{\text{Si}}^\infty$  accurately since that value must be measured by a different sample from that for which a film thickness is to be measured. Where  $I_{\text{Si}}^\infty$  is to be measured using a separate sample, the uncertainties arising from instrument stability, and so on, are significantly higher than the contributions for the intensity ratios used in equations like Eqn (1). Hence the latter is almost universally used for measurements of thickness, rather than Eqn (7). Powell and Jablonski provide data for a spectrometer with an angle of  $54^\circ$  between the incident X-rays and the emitted Si 2p electrons. The calculations give the variation of  $L/\lambda$ , where  $\lambda$  is the inelastic mean free path. From these data, at an emission angle of  $50^\circ$  over the thickness range 0.2 to 4 nm, the maximum deviation from the result using a film-thickness-independent AL is 0.009 nm. For an emission angle of  $0^\circ$ , this maximum deviation increases to 0.016 nm. All the emission angles used here are well within this angular range. These calculations and those of the other 2001 publications<sup>23,24</sup> are all consistent and were made using an algorithm based on a solution of the kinetic Boltzmann equation within the transport approximation available in Ref. 25. These calculations give predictions that are consistent with the present experimental data.

To make comparisons for the thicknesses calculated using the thickness-dependent and thickness-independent ALs, we need to make an assumption concerning the behaviour of the intensity  $I_{\text{SiO}_2}$ . In the absence of calculations for  $I_{\text{SiO}_2}$ , we assume that the growth of this intensity and the decay of the substrate intensity are both characterised by the same value of  $L(d)$  for any thickness  $d$ , i.e. the EAL from Eqn (7) may be used in Eqn (1). This is in the spirit of the definition of EAL in ISO standards<sup>26,27</sup> which define EAL as a parameter which, when introduced in place of the inelastic mean free path into an expression derived for AES and XPS on the assumption that elastic-scattering effects are negligible for a given quantitative application, will correct that expression for elastic-scattering effects. Thus, for any given measurement of  $R$ ,

$$d(L) = \frac{L}{L_o} d(L_o) \quad (8)$$

where  $L_o$  is the constant AL of 2.996 nm and  $d(L_o)$  is the thickness derived from Eqn (1).

The first calculations of Powell and Jablonski<sup>22–24</sup> were made using the same elastic- and inelastic-scattering properties in the Si substrate as in the  $\text{SiO}_2$  overlayer and were prior

to the more recent upgrades of the NIST AL software<sup>28,29</sup> involving more accurate differential elastic-scattering cross sections<sup>30</sup> and prior to the release of the SESSA software.<sup>31</sup> Briefly, elastic scattering in the EAL Database, SRD 82,<sup>29</sup> is characterised by the transport mean free path that is used in an approximate algorithm while SESSA<sup>31</sup> utilises separate differential elastic-scattering cross sections for the substrate and overlayer film in a Monte Carlo simulation. The latter is expected to be more realistic than the transport approximation. SRD 82 uses the same scattering parameters for the overlayer and substrate. The 2001 data of Powell and Jablonski,<sup>22–24</sup> although consistent with our experimental data, have thus been superseded by later calculations.

Using recent<sup>30</sup> and the latest recent<sup>31</sup> software, Powell *et al.*<sup>32</sup> have provided calculations of the film-thickness-dependence of the EAL. The results of these calculations are shown in Fig. 7 for the analysis of SiO<sub>2</sub> on Si using Mg K $\alpha$  X-rays with emission angles of 25° and 34°. The absolute values of the EALs are not too important as they may be up to 20% in error and, additionally, they relate to measurements involving the total peak intensity including all shake-up and not just the peak after removal of the Shirley background as used here. In practice, it would actually be very difficult to measure the full intensity including the shake-up since the shake-up energy ranges for the elemental and oxide peaks fully overlap. The film-thickness-dependence of the EAL, however, is thought to be more accurate than the absolute values of the EALs and would, if valid, define the extent of the linearity of the XPS method. The curves are for the latest version of the NIST SRD 82<sup>29</sup> in which the overlayer and substrate still have the same elastic and inelastic scattering properties, whereas the plotted points are for the SESSA software system<sup>31</sup> where the overlayer and substrate have different properties. The SESSA-based calculations show the strongest dependence on the film thicknesses.

Using the format of Fig. 4, we may use the data in Fig. 7 to evaluate the thickness determined using XPS, calculated with a variable AL,  $d(L)$ , compared to the thickness calculated with a fixed AL,  $d(L_0)$ . The fixed value of  $L_0$  is chosen to be such that when  $d(L)$  is plotted *versus*  $d(L_0)$ , the result can be

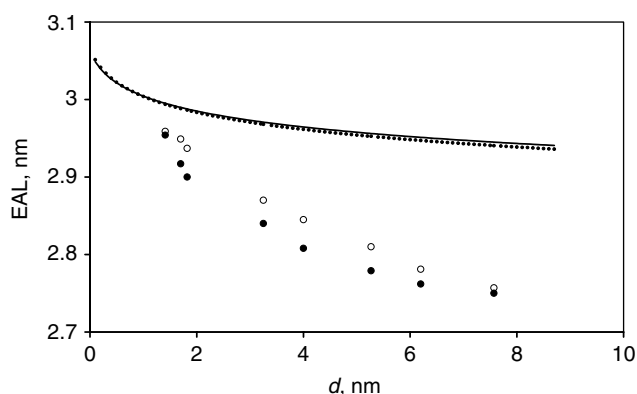


**Figure 7.** EALs<sup>32</sup> for SiO<sub>2</sub> on Si for XPS using Mg K $\alpha$  X-rays with 25° and 34° emission angles as a function of the film thickness,  $d$ . The data are from the use of Ref. 29: (·····) and (—), and Ref. 31: (○) and (●), for 25° and 34° emission angles, respectively.

fitted with a regression line of the form

$$d(L) = md(L_0) + c \quad (9)$$

with the gradient,  $m$ , set to unity. This follows the procedure for determining the calibration of the fixed value of  $L_0$  in the pilot study intercomparison.<sup>1</sup> We then evaluate the offset,  $c$ .

Figure 8(a) shows a plot of  $d(L)$  versus  $d(L_0)$  for the two sets of EALs shown in Fig. 7, from the SESSA software,<sup>31</sup> for the 0 to 4-nm range of the current work. From the regression fits of straight lines to the calculated data for the 5 thicknesses shown for the SESSA calculations, the offsets  $c$  may be determined. These offsets are 0.092 and 0.103 nm, respectively. The EAL calculations for 25° and 34° emission angles for the overlayer and substrate with the same scattering properties from SRD 82 lead to smaller offsets,  $c$ , of 0.026 and 0.024 nm, respectively. If the regression fits are made over the wider 0–8 nm range, all these offsets increase to 0.145 and 0.129 nm for the layer and substrate with different scattering properties using SESSA and 0.036 and 0.032 nm for layer and substrate with the same scattering properties using SRD 82, respectively. Figure 8(b) shows the plot for the differences,  $d(L) - d(L_0)$ , for all four sets of EALs

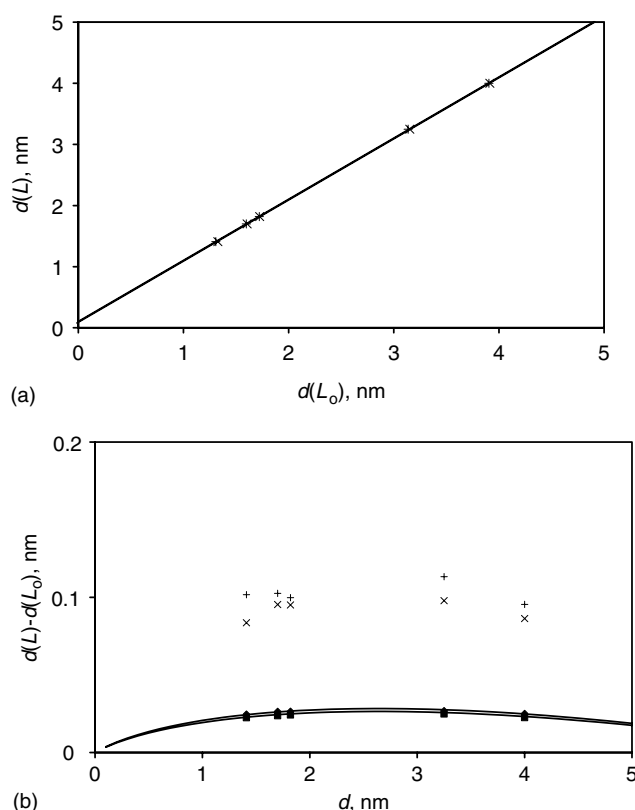


**Figure 8.** Results for the calculated EALs from Fig. 7, (a) the thickness for the film-thickness-dependent AL,  $d(L)$ , calculated using SESSA<sup>31</sup> versus the thickness for a fixed AL,  $d(L_0)$ , with  $L_0$  chosen to give a regression line of unity gradient, (b) the difference,  $d(L) - d(L_0)$ , as a function of the layer thickness. In (b), the continuous curve shows how the result for the calculations using SRD 82 version 1.1<sup>29</sup> will pass through the origin for 25° (◆) and 34° (□) emission angles. A similar curve, also passing through the origin, should occur for the SESSA<sup>31</sup> analysis at 25° (x) and 34° (+) emission angles.

to show how the individual data points lie in relation to the plot in Fig. 4. It is clear that the SRD 82 calculations for the layer and substrate with the same scattering properties are more consistent with the present experimental data and that the SESSA calculations are far removed from agreement with those data. It is not clear, now, if the calculated results for the overlayer and substrate scattering properties being similar should be used or if the more recent SESSA calculations need to be extended significantly further to incorporate, for instance, (i) specific additional surface effects that are thought to be strong in metals,<sup>10–13</sup> (ii) the intensity lost to shake-up that cannot be included experimentally for such close peaks, and (iii) the behaviour of the overlayer intensity. However, what is clear is that the fixed AL results used previously in the pilot study<sup>1</sup> are consistent with the present experimental data and the recently calculated film-thickness-dependencies of the ALs using SESSA, if used in Eqn (1), are not.

## CONCLUSIONS

The results reported here support the linearity of XPS as used with Eqns (2) to (6) and in the studies leading up to and within the CCQM pilot study<sup>1</sup> for SiO<sub>2</sub> on Si. Linearity has been exhibited for layers with thicknesses between 1.5 nm and 7.5 nm in the pilot study<sup>1</sup> and in this case from <0.03 nm up to 4 nm. The previously evaluated uncertainty in the linearity, of  $\pm 0.025$  nm, is consistent with the present work. This conclusion does not, of course, mean that thicknesses may be calculated with similar accuracies using a thickness-independent AL for other geometries or other material systems than those expressed in the present study. The  $\pm 0.025$  nm uncertainty was originally based partly on the 2001 calculations of the film-thickness-dependence of the EALs by Powell and Jablonski using SRD 82. The most recent calculations by Powell and co-workers using SESSA predict a much stronger non-linearity that is not supported by the present measurements.

## Acknowledgements

The authors would like to thank S. J. Spencer for his analysis of the data and preparing the figures, and C. J. Powell and W. S. M. Werner for their helpful comments and a preprint of Ref. 32. This research was partially supported by the Ministry of Commerce, Industry and Energy, Korea, through system IC 2010 project and partly through the Valid Analytical Measurement Programme supported by the National Measurement Policy Unit of the UK Department of Trade and Industry.

## REFERENCES

1. Seah MP, Spencer SJ, Bensebaa F, Vickridge I, Danzebrink H, Krumrey M, Gross T, Oesterle W, Wendler E, Rheinländer B, Azuma Y, Kojima I, Suzuki N, Suzuki M, Tanuma S, Moon DW, Lee HJ, Cho HM, Chen HY, Wee ATS, Osipowicz T, Pan JS, Jordaan WA, Hauert R, Klotz U, van der Marel C, Verheijen M, Tamminga Y, Jeynes C, Bailey P, Biswas S, Falke U, Nguyen NV, Chandler-Horowitz D, Ehrstein JR, Muller D, Dura JA. *Surf. Interface Anal.* 2004; **36**: 1269.
2. Seah MP. *Surf. Interface Anal.* 2005; **37**: 300.
3. Seah MP, Spencer SJ. *Surf. Interface Anal.* 2005; **37**: 731.
4. Cumpson PJ. *Surf. Interface Anal.* 2000; **29**: 403.
5. Seah MP, Spencer SJ. *Surf. Interface Anal.* 2002; **33**: 640.
6. Tanuma S, Powell CJ, Penn DR. *Surf. Interface Anal.* 1994; **21**: 165.
7. Seah MP, Gilmore IS. *Surf. Interface Anal.* 2001; **32**: 835.
8. Powell CJ, Jablonski A. *J. Phys. Chem. Ref. Data* 1999; **28**: 19.
9. Powell CJ, Jablonski A. *J. Electron Spectrosc. Relat. Phenom.* 2001; **114–116**: 1139.
10. Feibelman PJ. *Surf. Sci.* 1973; **36**: 558.
11. Kwei CM, Wang CY, Tung CJ. *Surf. Interface Anal.* 1998; **26**: 682.
12. Werner WSM. *Surf. Sci.* 2005; **588**: 26.
13. Pauly N, Tougaard S, Yubero F. *Surf. Interface Anal.* 2005; **37**: 1151.
14. Seah MP, Spencer SJ. *J. Vac. Sci. Technol. A* 2003; **21**: 345.
15. Kim KJ, Park KT, Lee JW. *Thin Solid Films* 2006; **500**: 356.
16. Saha C, Dao S, Ray SK, Lahiri SK. *J. Appl. Phys.* 1998; **83**: 4472.
17. Kim KJ, Moon DW. *Surf. Interface Anal.* 1998; **26**: 9.
18. Hollinger G, Himpsel FJ. *Appl. Phys. Lett.* 1984; **44**: 93.
19. Keister JW, Rowe JE, Kolodziej JJ, Ntini H, Tao H-S, Madey TE, Lucovsky G. *J. Vac. Sci. Technol. A* 1999; **17**: 1250.
20. Shirley DA. *Phys. Rev., B* 1972; **5**: 4709.
21. Seah MP, Spencer SJ. *Surf. Interface Anal.* 2003; **35**: 515.
22. Powell CJ, Jablonski A. *J. Vac. Sci. Technol. A* 2001; **19**: 2604.
23. Powell CJ, Jablonski A. *J. Electron Spectrosc.* 2001; **114–116**: 1139.
24. Powell CJ, Jablonski A. *Surf. Sci. Lett.* 2001; **488**: L547.
25. Powell CJ, Jablonski A. *NIST Electron Effective-Absorption-Length Database*, SRD 82, Version 1.0. National Institute of Standards and Technology: Gaithersburg, MD, 2001.
26. ISO181152001:Amd2, draft, ISO, Geneva, 2007.
27. Powell CJ, Jablonski A. *Surf. Interface Anal.* 2002; **33**: 211.
28. Jablonski A, Salvat F, Powell CJ. *J. Phys. Chem. Ref. Data* 2004; **33**: 409.
29. Powell CJ, Jablonski A. *NIST Electron Effective-Absorption-Length Database*, SRD 82, Version 1.1. National Institute of Standards and Technology: Gaithersburg, MD, 2003; <http://www.nist.gov/srd/nist82.htm>.
30. Jablonski A, Salvat F, Powell CJ. *NIST Electron Elastic-Scattering Cross-Section Database*, Version 3.1. National Institute of Standards and Technology: Gaithersburg, MD, 2003; <http://www.nist.gov/srd/nist64>.
31. Werner W, Smekal W, Powell CJ. *NIST Database for the Simulation of Electron Spectra for Surface Analysis*, SRD 100, Version 1.0. National Institute of Standards and Technology: Gaithersburg, MD, 2005; <http://www.nist.gov/srd/nist100.htm>.
32. Powell CJ, Werner WSM, Smekal W. *Appl. Phys. Lett.* (in press).